Numerical studies on the spherically expanding premixed cool flames under gravitational conditions

Yiqing Wang[1], Xuefeng Guan[1], Shumeng Xie[1], Mengni Zhou[2], Zunhua Zhang[2], Zheng Chen[3], Tianhan Zhang[1]
[1]Department of Mechanics and Aerospace Engineering, Southern University of Science and Technology
Shenzhen, Guangdong, PR China
[2]School of Naval Architecture, Ocean and Energy Power Engineering, Wuhan University of Technology
Wuhan, Hubei 430063, PR China
[3]SKLTCS, CAPT, BIC-ESAT, College of Engineering, Peking University
Beijing, 100871, PR China

1 Introduction

Cool flame has received renewed interest in recent years due to the critical role of low-temperature chemistry in the advanced engine [1, 2], where the low-temperature ignition and cool flames significantly affect the combustion processes, including the engine ignition timing, flame propagation, fuel consumption, and heat release rate.

The experimental studies on cool flames have been performed in various flame geometries, including heated burners [3], jet-stirred reactors [4], heated flow reactors [5, 6], counterflow burners [7-9] and so on. However, only a few studies have focused on cool flame laminar speed measurements. Laminar flame speed (LFS) is a fundamental physicochemical property of a combustible mixture [10]. Regarding hot flame and high-temperature chemistry (HTC), LFS has been widely used to validate the chemical kinetic model and characterize the heat release rate and diffusive transport coupling [11].

Belmont and co-workers [12, 13] used the laminar flat flame Hencken burner for cool flame speed measurements, where a laminar and freely-propagating cool flame was isolated and stabilized through the suppression of trailing hot flame. These experiments were conducted at low-pressure conditions with ozone addition, which might mitigate or perturb the chemistry-transport coupling. Recently, Susa et el. [14, 15] measured the flame speed at high-temperature conditions by igniting a spherically expanding flame in the shock tube. They reported the so-called 'multistage flame' structures and non-monotonic dependence of the 'hot' flame speed on the temperature within the negative temperature coefficient (NTC) region. Based on the numerical simulations considering detailed chemistry, Zhang et al. [16-18] demonstrated that this abnormal NTC behavior of flame speed is attributed to the occurrence of autoignition-assisted cool flame. Still, the pure premixed cool flame speed remains a challenge for experimentalists.

Correspondence to: zhangth@sustech.edu.cn

For hot flame laminar speed measurement, a spherical bomb is widely used due to the advantages of simple configuration and a well-defined stretch rate. Previous studies on hot flames suggested that a minimum LFS of 15 cm/s for flames is required to avoid the strong flame shape deformation and thus reach accurate measurements under a normal gravity [19, 20]. Whether the 15 cm/s speed criterion applies to the cool flame measurement is questionable since the thermal expansion of cool flames is much smaller than hot flames, which would substantially reduce the influence of buoyancy.

Based on the above discussion, the objective of this work is to identify the effects of buoyancy on the propagation of spherically expanding cool flames so as to evaluate the suitability of the spherically expanding flame method on cool flame speed measurements. In the current work, the spherical DME/air cool flames propagating in a closed vessel are numerically studied through 2-D simulations considering detailed chemistry. DME is considered here as in many previous numerical studies [21, 22] due to its well-established, compact kinetic mechanisms for low-temperature chemistry. The present study is expected to shed light on cool flame speed measurement and thus help to improve the understanding of low-temperature chemistry and cool flame propagation.

2 Numerical model and methods

We consider the transient cool flame ignition and propagation of DME/air mixtures in a closed cylindrical vessel of radius R_W=10 cm. As shown in Fig. 1, the flame is ignited by a hot spot with the radius of R_H and temperature of T_H at the center (i.e., r=0 and $z = R_W$). T_H is varied to ignite the cool flame, while R_H=2 mm is used throughout this work. The DME/air mixture with an equivalence ratio of ϕ is initially quiescent at unburned temperature T_0 and pressure P_0. The 2-D computational domain has a radius of R_W and a length of $2R_W$. The wall boundary condition is applied on the top, down, and right sides, while the left side is the axis of symmetry. The gravity vector is co-aligned with the z direction.

The OpenFOAM-based [23] solver EBIdnsFoam, which was developed by Zirwes et al. [24], is used to simulate the 2-D cool flame propagation. In EBIdnsFOAM, the compressible Navier-Stokes is solved using the finite volume method in cylindrical coordinates. The open-source library Cantera [25] is incorporated to calculate chemical kinetics, thermodynamic, and transport properties. The mixture-averaged transport model is employed without the consideration of Soret diffusion. The radiation effect is neglected. Considering the large simulation domain (i.e., 10 cm × 20 cm) and long simulation time (on the order of 0.5 s), these 2-D simulations are computationally expensive. To this end, the dynamic load balancing algorithm developed by Tekgül et al. [26] is integrated to balance the chemistry load and thus accelerate the calculation of reaction rates. In addition, the load-balanced 2-D adaptive mesh refinement technique developed by Rettenmaier et al. [27] is also adopted for efficiency. Based on the normalized temperature gradient, a 3-level AMR with a minimum mesh size of 64 μm is used. The grid convergence is ensured. The DME oxidation is modeled by a 39-species skeletal mechanism [28, 29] which includes both the low-temperature and high-temperature chemistry. This mechanism has been used in many previous studies [21, 22].

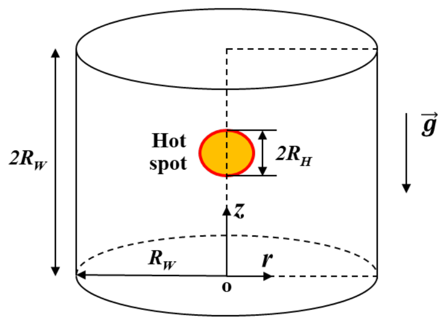

Figure 1: Schematics of the simulation configuration.

In the spherically expanding flame method, the flame radius history $R_f = R_f(t)$ is recorded to derive the LFS. Usually, it is assumed that the burned gas inside the spherical flame front is static, and thus the stretched flame speed with respect to the burned gas is $S_b = \mathrm{d}R_f/\mathrm{d}t$. Then, the unstretched flame speed with respect to the burned gas S_b^0 can be obtained from extrapolation based on the following linear model [30]:

$$S_b = S_b^0 - L_b K$$

where $K = (2/R_f)(\mathrm{d}R_f/\mathrm{d}t)$ is the flame stretch rate, and L_b is the Markstein length relative to the burned gas. Knowing S_b^0, the unstretched flame speed for the unburned gas S_u^0, i.e., the LFS, can be deduced from the mass conservation: $S_u^0 = \sigma S_b^0$ where $\sigma = \rho_b/\rho_u$ is the density ratio between the burned gas (at equilibrium state) and unburned gas. Unlike hot flames, the temperature and density in the burned gas of cool flames vary with time due to the high-temperature chemistry reactivity. Therefore, S_b^0 is utilized to characterize the cool flame speed in order to circumvent the ambiguous definition of σ. In our simulations, the flame radius R_f is defined by the temperature iso-surface with the value at the maximum heat release rate position in the corresponding 1-D planar freely-propagating cool flame modeled by Cantera. To avoid impacts of the unsteady ignition process and chamber confinement, only data within the range of 0.5 cm < R_f < 2 cm is used to extract S_b^0.

3 Results and discussion

Two groups of cool flames with varying T_0 and ϕ are considered to yield different cool flame speeds. In the first group, five cool flames with different T_0 ranging from 400 K to 550 K are considered; in the second group, another five cool flames with different ϕ ranging from 0.3 to 4.0 are considered. The parameters for the ten cases (Case 4 and Case 9 are identical) are listed in the head of Fig. 2 from left to right. It can be seen that S_b^0 covers a wide range spanning from 6.4 cm/s to 18.8 cm/s. The effects of buoyancy on the spherically expanding flames can be characterized by the Richardson number, Ri, defined as [31] :

$$Ri = \frac{(\rho_u - \rho_b)}{\rho_u} \frac{g R_{eq,V}}{\left(S_b^0\right)^2}$$

where ρ_u and ρ_b denote the density of the unburned and burned gas in the corresponding 1D freely propagating cool flame, g the gravitational acceleration, $R_{eq,V}$ is the equivalent radius obtained from the sphere with the same volume as the flame volume V_f . V_f can be computed by integrating the volume surrounded by the flame front (i.e., the temperature iso-surface) in 3-D space. If Ri is sufficiently large, the buoyancy effect largely determines the flame motion.

Figure 2 shows the temporal evolution of flame shapes for these cool flames propagating in a gravitational environment. Ri characterizes the variation in time. For the slowly propagating cool flames, e.g., Cases 1, 3, and 6, the buoyancy effects substantially deform the flame shape. Initially, the flames possess a spherical shape. As Ri increases, the bottom side of the flames becomes flat, and eventually, the lower part forms a mushroom-like shape as it could not propagate downwardly against the flow induced by buoyancy. Specifically, the flame upward motion induces entrainment of the unburned gas from the bottom of the flame, leading to the formation of a toroidal vortex in the vicinity of the outer horizontal part of the flame. This eventually results in a cusp forming the flame's inner bottom side at Ri= 22. In comparison, the buoyancy effect is much weak for cool flames with high propagating speeds as they expand in a spherical manner from beginning to end.

Figure 3 (left) shows the derived S_b-K curves based on these three techniques for Case 1, where the mushroom-like flame shape is observed. It can be seen that the S_b-K curves based on R_h and $R_{eq,CR}$ do not reveal a linear trend after the transient ignition stage, where R_h and $R_{eq,CR}$ represent the equivalent flame radius obtained from the most outer horitonal distance and the 2-D cross area of the flame front, respectively. Compared to R_h and $R_{eq,CR}$, the S_b-K curve based on $R_{eq,V}$ exhibits relatively better linearity, although the S_b from $R_{eq,V}$ is systematically higher than $R_{f,0g}$. As a result, the extrapolated S_b^0 from $R_{eq,V}$ is approximately 20% higher than that from $R_{f,0g}$ (7.8 cm/s vs. 6.4 cm/s). Note that $R_{f,0g}$ is defined as the position where the local temperature corresponds to the maximum heat release rate in 1D planar cool flame.

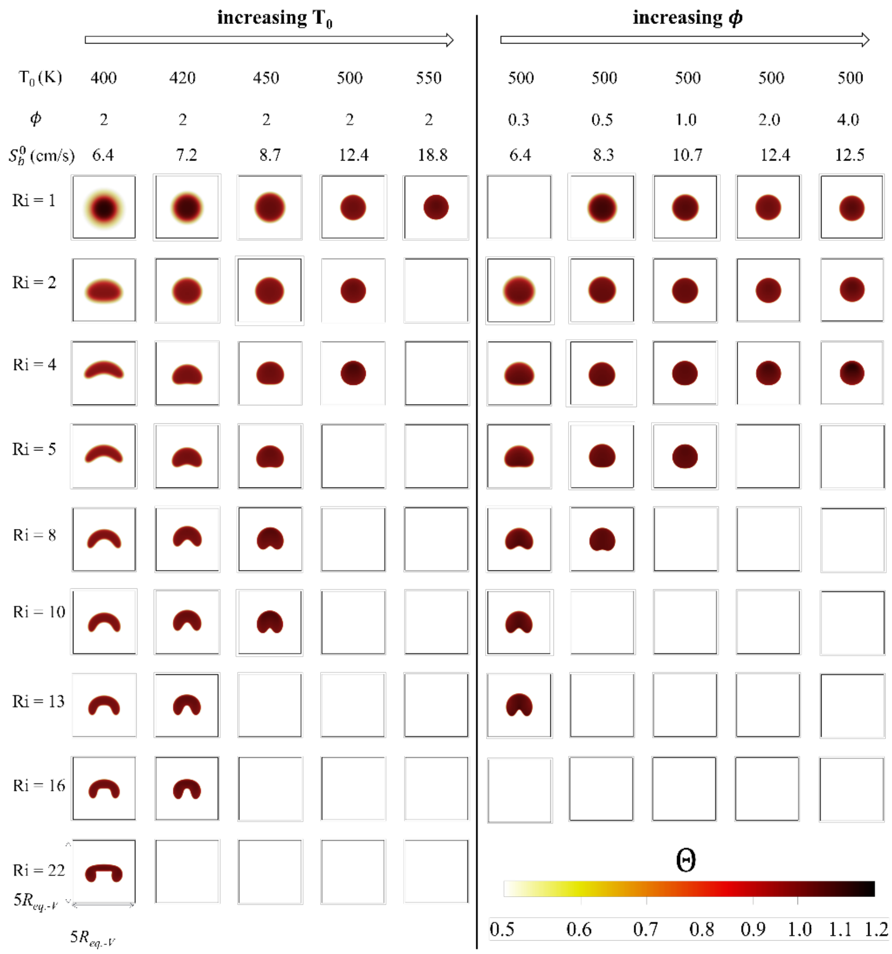

Figure 2: Flame shapes for all cases at different Richardson numbers Ri. For each panel, the corresponding T_0, ϕ and S_b^0 are also provided. The colorbar shows the normalized temperature field $\Theta = (T - T_0)/(T_{\max} - T_0)$. The spatial coordinates are normalized by the $R_{eq,V}$ to better depict the flame shape.

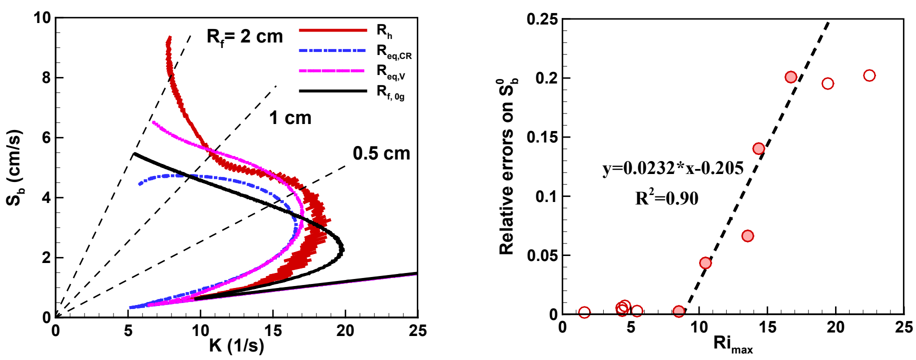

Figure 3: Left: S_b–K curves based on a different equivalent radius for Case 1. The results from the corresponding 1-D spherical cool flames without buoyancy ($R_{f,0g}$) are also plotted for comparison. Right:

The relative errors between S_b^0 obtained from $R_{eq,V}$ and $R_{f,0g}$ for all cases. The data points represented by the red circles with filled color are selected for linear fitting.

Finally, Figure 3 (right) summarizes the relative errors between S_b^0 obtained from $R_{eq,V}$, and $R_{f,0g}$ for all cases as a function of $Ri_{\max}$, which is determined by substituting R_f=2 cm into the expression for Ri. It can be seen that the relative errors of S_b^0 follow the piece-wise linear function of $Ri_{\max}$. When $Ri_{\max}$<8, the relative errors remain negligible. In this context, it can be concluded that under gravitational conditions, the buoyant spherical cool flames can still be utilized to measure the cool flame speed with sufficient accuracy as long as the corresponding $Ri_{\max}$<10 or S_b^0>8 cm/s.

4 Conclusions

In this study, 2-D numerical simulations with detailed DME/air chemistry are performed to investigate the propagation of spherically expanding cool flames under gravitational conditions. It is found that for slowly propagating cool flames, the initially spherical flame shape evolves into a mushroom-like shape due to buoyancy effects. Nevertheless, the unstretched cool flame speed can still be accurately extrapolated based on the 3-D flame volume method at S_b^0>8 cm/s. The current work provides guidance for the terrestrial experiment design to measure cool flame speed using a spherical bomb.

Acknowledgements

This work was supported by National Natural Science Foundation of China (No. 52176096). We thank Drs. Thorsten Zirwes, Feichi Zhang, and Henning Bockhorn at Karlsruhe Institute of Technology for providing us with their EBI-DNS code. We also acknowledge the computing resources provided by the Center for Computational Science and Engineering of the Southern University of Science and Technology.

References

[1] J.E. Dec, Advanced compression-ignition engines—understanding the in-cylinder processes, Proc. Combust. Inst. 32 (2009) 2727-2742.

[2] S.L. Kokjohn, R.M. Hanson, D.A. Splitter, R.D. Reitz, Fuel reactivity controlled compression ignition (RCCI): a pathway to controlled high-efficiency clean combustion, Int. J. Engine Res. 12 (2011) 209-226.

[3] F.W. Williams, R.S. Sheinson, Manipulation of Cool and Blue Flames in the Winged Vertical Tube Reactor, Combust. Sci. Technol. 7 (1973) 85-92.

[4] O. Herbinet, F. Battin-Leclerc, Progress in Understanding Low-Temperature Organic Compound Oxidation Using a Jet-Stirred Reactor, Int. J. Chem. Kinet. 46 (2014) 619-639.

[5] F.L. Dryer, F.M. Haas, J. Santner, T.I. Farouk, M. Chaos, Interpreting chemical kinetics from complex reaction–advection–diffusion systems: Modeling of flow reactors and related experiments, Prog. Energy Combust. Sci. 44 (2014) 19-39.

[6] H. Oshibe, H. Nakamura, T. Tezuka, S. Hasegawa, K. Maruta, Stabilized three-stage oxidation of DME/air mixture in a micro flow reactor with a controlled temperature profile, Combust. Flame 157 (2010) 1572-1580.

[7] W. Sun, S.H. Won, Y. Ju, In situ plasma activated low temperature chemistry and the S-curve transition in DME/oxygen/helium mixture, Combust. Flame 161 (2014) 2054-2063.

[8] S. Deng, P. Zhao, D. Zhu, C.K. Law, NTC-affected ignition and low-temperature flames in nonpremixed DME/air counterflow, Combust. Flame 161 (2014) 1993-1997.

[9] C.B. Reuter, S.H. Won, Y. Ju, Experimental study of the dynamics and structure of self-sustaining premixed cool flames using a counterflow burner, Combust. Flame 166 (2016) 125-132.

[10] C.K. Law, Combustion physics, Combustion physics2006.
[11] F.N. Egolfopoulos, N. Hansen, Y. Ju, K. Kohse-Höinghaus, C.K. Law, F. Qi, Advances and challenges in laminar flame experiments and implications for combustion chemistry, Prog. Energy Combust. Sci. 43 (2014) 36-67.
[12] M. Hajilou, M.Q. Brown, M.C. Brown, E. Belmont, Investigation of the structure and propagation speeds of n-heptane cool flames, Combust. Flame 208 (2019) 99-109.
[13] M. Hajilou, T. Ombrello, S.H. Won, E. Belmont, Experimental and numerical characterization of freely propagating ozone-activated dimethyl ether cool flames, Combust. Flame 176 (2017) 326-333.
[14] A.M. Ferris, A.J. Susa, D.F. Davidson, R.K. Hanson, High-temperature laminar flame speed measurements in a shock tube, Combust. Flame 205 (2019) 241-252.
[15] A.J. Susa, A.M. Ferris, D.F. Davidson, R.K. Hanson, Experimental Observation of Negative Temperature Dependence in iso-Octane Burning Velocities, AIAA J. 57 (2019) 4476-4481.
[16] T. Zhang, A.J. Susa, R.K. Hanson, Y. Ju, Studies of the dynamics of autoignition assisted outwardly propagating spherical cool and double flames under shock-tube conditions, Proc. Combust. Inst. 38 (2021) 2275-2283.
[17] T. Zhang, Y. Ju, Structures and propagation speeds of autoignition-assisted premixed n-heptane/air cool and warm flames at elevated temperatures and pressures, Combust. Flame 211 (2020) 8-17.
[18] T. Zhang, A.J. Susa, R.K. Hanson, Y. Ju, Two-dimensional simulation of cool and double flame formation induced by the laser ignition under shock-tube conditions, Proc. Combust. Inst., doi:https://doi.org/10.1016/j.proci.2022.08.068(2022).
[19] P.D. Ronney, H.Y. Wachman, Effect of gravity on laminar premixed gas combustion I: Flammability limits and burning velocities, Combust. Flame 62 (1985) 107-119.
[20] Z. Chen, On the accuracy of laminar flame speeds measured from outwardly propagating spherical flames: Methane/air at normal temperature and pressure, Combust. Flame 162 (2015) 2442-2453.
[21] Q. Yang, P. Zhao, Minimum ignition energy and propagation dynamics of laminar premixed cool flames, Proc. Combust. Inst. 38 (2021) 2315-2322.
[22] Y. Wang, W. Han, T. Zirwes, F. Zhang, H. Bockhorn, Z. Chen, Effects of low-temperature chemical reactions on ignition kernel development and flame propagation in a DME-air mixing layer, Proc. Combust. Inst., (2022).
[23] H.G. Weller, G. Tabor, H. Jasak, C. Fureby, A tensorial approach to computational continuum mechanics using object-oriented techniques, Comput. Phys. 12 (1998) 620-631.
[24] T. Zirwes, F. Zhang, P. Habisreuther, M. Hansinger, H. Bockhorn, M. Pfitzner, D. Trimis, Quasi-DNS dataset of a piloted flame with inhomogeneous inlet conditions, Flow Turbul. Combust. 104 (2020) 997-1027.
[25] D.G. Goodwin, H.K. Moffat, R.L. Speth, Cantera: An object-oriented software toolkit for chemical kinetics, thermodynamics, and transport processes. Version 2.3.0, Cantera Developers, Warrenville, IL, (2017).
[26] B. Tekgül, P. Peltonen, H. Kahila, O. Kaario, V. Vuorinen, DLBFoam: An open-source dynamic load balancing model for fast reacting flow simulations in OpenFOAM, Computer Physics Communications 267 (2021) 108073.
[27] D. Rettenmaier, D. Deising, Y. Ouedraogo, E. Gjonaj, H. De Gersem, D. Bothe, C. Tropea, H. Marschall, Load balanced 2D and 3D adaptive mesh refinement in OpenFOAM, SoftwareX 10 (2019) 100317.
[28] Z. Zhao, M. Chaos, A. Kazakov, F.L. Dryer, Thermal decomposition reaction and a comprehensive kinetic model of dimethyl ether, Int. J. Chem. Kinet. 40 (2008) 1-18.
[29] A. Bhagatwala, Z. Luo, H. Shen, J.A. Sutton, T. Lu, J.H. Chen, Numerical and experimental investigation of turbulent DME jet flames, Proc. Combust. Inst. 35 (2015) 1157-1166.
[30] P. Clavin, Dynamic behavior of premixed flame fronts in laminar and turbulent flows, Prog. Energy Combust. Sci. 11 (1985) 1-59.
[31] L. Berger, R. Hesse, K. Kleinheinz, M.J. Hegetschweiler, A. Attili, J. Beeckmann, G.T. Linteris, H. Pitsch, A DNS study of the impact of gravity on spherically expanding laminar premixed flames, Combust. Flame 216 (2020) 412-425.